Acta Crystallographica Section D
Biological Crystallography
ISSN 0907-4449

The mechanism of iron uptake by transferrins: the X-ray structures of the 18 kDa NII domain fragment of duck ovotransferrin and its nitrilotriacetate complex

Paula Kuser,[a]† David R. Hall,[b]‡ Mei Ling Haw,[a,c] Margarete Neu,[b]§ Robert W. Evans[c] and Peter F. Lindley[a,b]*¶

[a]Department of Crystallography, Birkbeck College, University of London, Malet Street, London WC1E 7HX, England, [b]CLRC Daresbury Laboratory, Warrington, Cheshire WA4 4AD, England, and [c]Metalloprotein Research Group, Division of Biomolecular Sciences, The Randall Centre for Molecular Mechanisms of Cell Function, King's College London, 3.6A New Hunt's House, Guy's Campus, London SE1 1UL, England

† Current address: Laboratório Nacional de Luz Síncrotron, Caixa Postal 6192, CEP 13084-971, Campinas, SP, Brazil.
‡ Current address: Molecular Enzymology Group, Cancer Research UK, Clare Hall, South Mimms, Hertfordshire EN6 3LD, England.
§ Current address: GlaxoSmithKline, Department of Computational and Structural Science, Research Centre, Gunnels Wood Road, Stevenage, Hertfordshire SG1 2NY, England.
¶ Current address: European Synchrotron Radiation Facility, 6 Rue Horowitz, F-38043 Grenoble CEDEX, France.

Correspondence e-mail: lindley@esrf.fr

Received 17 December 2001
Accepted 26 February 2002

PDB References: 18 kDa NII domain fragment of duck ovotransferrin, 1gv8, r1gv8sf; NTA complex, 1gvc, r1gvcsf.

In a previous paper [Lindley *et al.* (1993), *Acta Cryst.* D**49**, 292–304], the X-ray structure analysis of the 18 kDa fragment of duck ovotransferrin, corresponding to the NII domain of the intact protein, was reported at a resolution of 2.3 Å. In this structure, the Fe^{III} cation binds to two tyrosine residues and the synergistic carbonate anion in an identical manner to that found in the intact protein. However, the aspartate and histidine residues, normally involved in iron binding in transferrins, are absent in the fragment and it was not possible to unequivocally define what had replaced them. The electron density was tentatively assigned to be a mixture of peptides, presumably resulting from the proteolytic preparation of the fragment, binding to the iron through their amino and carboxylate termini. A more recent X-ray analysis of the fragment, from a different preparation, has resulted in a structure at 1.95 Å, in which glycine appears to be the predominant residue bound to the cation. In an alternative attempt to clarify the binding of iron to the 18 kDa fragment, the metal was removed by dialysis and replaced in the form of ferric nitrilotriacetate. Crystallization of this complex has resulted in an X-ray structure at 1.90 Å in which the Fe^{III} is bound to the synergistic carbonate anion and only one tyrosine residue in a manner almost identical to the intact protein. The carboxylate groups and the tertiary amino group of the nitrilotriacetate occupy the remaining coordination sites. The second tyrosine residue, Tyr95, is not bound directly to the iron. The implication of these structures with respect to the mechanism of iron binding by the transferrins is addressed.

1. Introduction

The transferrin family of proteins plays a central role in the iron metabolism of vertebrates and some invertebrates (for recent reviews, see Aisen, 1998; Arnesano & Provenzani, 2001; Crichton, 2001; Lindley, 2001; Smith, 2001). Serum transferrin has the specific role of iron transport and delivers Fe^{III}, virtually insoluble at physiological pH, to reticulocytes by means of receptor-mediated endocytosis (Jandl *et al.*, 1959). The transferrin molecule comprises two structurally homologous lobes, each containing two dissimilar domains, with the metal-binding site in each lobe located deep within the inter-domain cleft. Such a structure is consistent with a 'Venus fly-trap' mechanism for metal uptake and release and a comparison of the X-ray structures of iron-loaded and apo transferrins, together with solution-scattering studies, has confirmed that gross conformational changes occur on iron binding and release. Kinetic studies where the iron is added to the apo transferrin in the form of a metal chelate have enabled

a number of key stages to be identified in the formation of a metal–anion–transferrin ternary complex (Aisen & Leibman, 1973; Cowart *et al.*, 1982). The initial stage involves the binding of the synergistic carbonate anion to a lobe of the apo transferrin in the open form. This is followed by stages involving a partial detachment of the ligands of the added metal chelate, the formation of a transferrin–anion–metal–chelate quaternary complex and the complete detachment of the chelating ligands from the iron. In the final stage domain closure leads to the specific transferrin–anion–metal complex.

Strong evidence for such a mechanism was provided by the X-ray structure determination of an 18 kDa quarter molecule of duck ovotransferrin (dOT) corresponding to the second domain in the N-terminal lobe (Lindley *et al.*, 1993). In this structure, the Fe^{III} is bound to the synergistic carbonate anion and two tyrosine residues, Tyr95 and Tyr194 (equivalent to Tyr188 in the sequence of human serum transferrin, hST), in an almost identical manner to that found in the intact N-terminal lobe. However, the 18 kDa fragment lacks two of the residues that normally coordinate to the metal, namely Asp63 (located in domain I of the intact protein) and His249 (hST numbering), located on the second inter-domain strand linking domains I and II in the intact protein. The electron density in the structure determined at 2.3 Å resolution clearly showed that these ligands had been replaced, but was not of sufficient quality to show unequivocally what had replaced them. The most likely explanation seemed to be a mixture of polypeptides, arising from the proteolytic method of preparation, binding to the iron through their amino- and carboxy-termini.

In this paper, the structure analysis of a fresh preparation of the 18 kDa fragment from dOT at a resolution of 1.95 Å is reported. This analysis indicates that a glycine residue is the predominant species bound to the metal. In a further experiment to clarify the nature of the iron environment in the 18 kDa fragment, the iron and its chelating ligands were removed with citrate and replaced in the form of ferric nitrilotriacetate. The structure of the resulting complex at 1.90 Å resolution provides further evidence for an intermediate quaternary transferrin–anion–metal–chelate complex. In addition, the complex suggests sequential roles for Tyr188 (hST numbering) and Tyr95 in metal binding.

2. Experimental

2.1. Preparation and crystallization of the 18 kDa NII domain fragment of dOT and its complex with nitrilotriacetate (NTA)

The 18 kDa fragment of dOT was prepared by partial digestion of duck ovotransferrin with immobilized subtilisin Carlsberg (Sigma Protease type VIII from *Bacillus lichenformis*, No. P5380), essentially using the procedure described by Evans & Madden (1984). However, instead of digestion at 277 K for 72 h, a batch method was employed where the reaction time was reduced to 24 h. This gave more reproducible results and a yield of the 18 kDa fragment of some 15–20% of the theoretical yield. Crystals of the fragment were grown in sitting drops at 277 K. The protein solution was buffered at pH 7.8 with 50 m*M* Tris–HCl and the precipitant solution contained 23% methanepentanediol. Sitting drops contained 25 µl of the fragment at concentrations between 20 and 40 mg ml^{-1} and 25 µl of precipitant. Yellow–orange lath-shaped crystals appeared between 1 and 4 weeks and sometimes longer.

The NTA complex was prepared from the 18 kDa fragment, firstly by removing the iron with 0.1 *M* citrate buffer at pH 4.7, when the apo fragment appears colourless. The pH was then adjusted with 50 m*M* Tris to 7.8 and ferric nitrilotriacetate solution added. The 18 kDa fragment immediately turns pink. Excess Fe–NTA was then removed by concentrating the solution and adding more 50 m*M* Tris at pH 7.8. This protocol can also be used to bind other ferric complexes and other metals. Crystals of the 18 kDa NTA complex were then obtained in a similar manner to those of the 18 kDa fragment.

Table 1
Details of data collection and processing.

Values in parentheses correspond to the outermost resolution shell; 2.02–1.95 Å and 1.97–1.90 Å for the 18 kDa fragment and the NTA complex, respectively.

	18 kDa fragment	NTA complex
Wavelength (Å)	0.88	0.88
Detector	Rigaku R-AXIS II	Rigaku R-AXIS II
Resolution (Å)	27.22–1.95	26.92–1.90
Space group	$P3_1$	$P3_1$
Unit-cell parameters		
a (Å)	41.39	41.41
c (Å)	81.57	81.45
Redundancy	3.1 (2.3)	4.3 (2.1)
No. of observations	33700	52160
No. of unique (*hkl*)	11119	12081
Completeness	97.6 (94.5)	98.0 (97.3)
R_{merge}	0.055 (0.103)	0.041 (0.088)
$I/\sigma(I)$	6.6 (5.8)	8.5 (7.6)

2.2. X-ray data collection

Diffraction data for both structures were collected from capillary-mounted crystals at station 9.6 at the SRS, Daresbury Laboratory as indicated in Table 1. In each case, data were collected at a temperature of 277 K and the diffraction intensities fell away sharply at the resolution limit; attempts to flash-freeze crystals resulted, at best, in an unacceptable increase in the mosaicity. The data were integrated, scaled and merged using *MOSFLM* (Leslie, 1991), *ROTAVATA* and *AGROVATA* (from the *CCP*4 suite; Collaborative Computational Project, Number 4, 1994), respectively. The Matthews coefficient, V_M (Matthews, 1968), for the 18 kDa fragment and its NTA complex is 2.24 $Å^3\ Da^{-1}$ assuming that the asymmetric units contain a monomer; this value corresponds to a solvent content of about 45%. Wilson plots gave average thermal coefficients of 26 and 29 $Å^2$ for the 18 kDa fragment and the NTA complex, respectively.

Table 2
Refinement and model geometry statistics.

G factor and Ramachandran analysis were determined by *PROCHECK* (Laskowski *et al.*, 1993).

	18 kDa fragment	NTA complex
Amino acids	159	157
Protein atoms	1213	1204
Solvent atoms	115	95
Other molecules	Fe^{3+}, CO_3^{2-}, Gly	Fe^{3+}, CO_3^{2-}, NTA
Resolution limits (Å)	27.22–1.95	26.92–1.90
Working set *R* (observations)	0.169 (10587)	0.185 (11481)
Test set *R* (observations)	0.218 (532)	0.211 (573)
Cruickshank's DPI†	0.17	0.17
Average isotropic thermal parameters (Å^2)		
All atoms	32.8	34.7
Protein atoms	31.7	33.9
Main chain	30.1	32.3
Side chain	33.6	35.6
Solvent	43.8	45.2
Residues with poor main- and side-chain density	Glu144, Gly145, Ile146, Glu147, Ser148, Gly149	Ala251, Ala252, Glu144, Gly145, Ile146, Glu147, Ser148
Residues with incomplete side-chain density	His137, Lys205, Arg249	Lys103, His137, Trp143, Lys172, Lys182, Arg187, Lys224, Asp225, Lys243, Arg249
Residues in dual conformations	Asn188	Asn188
Distance deviations‡		
Bond distances (Å)	0.021	0.013
Bond angles (°)	1.93	1.68
Planar groups (Å)	0.008	0.006
Chiral volume deviation (Å^3)	0.118	0.118
Overall *G* factor	−0.03	0.00
Ramachandran analysis§ (%)		
Favourable	87.5 (119)	86.6 (116)
Additional	12.5 (17)	12.7 (17)
Generous	0.0 (0)	0.7 (1)
Disallowed	0.0 (0)	0.0 (0)

† Cruickshank (1996). ‡ R.m.s. deviations from standard values. § Values in parentheses are the numbers of residues in each region.

2.3. Structure solution and refinement

In the case of the 18 kDa fragment, Fourier syntheses ($2|F_o| - |F_c|$ and $|F_o| - |F_c|$) were computed with coefficients derived from the 1.95 Å resolution data and phases computed from the model at 2.3 Å (Lindley *et al.*, 1993). The coordination at the cation site was left incomplete, with only Tyr95, Tyr194 (Tyr188 in human serum transferrin numbering) and the carbonate anion bound to the iron being included in the model. However, the residual electron density in both syntheses could clearly be interpreted in terms of a glycine residue bound to the iron. This new model was then refined using the program *REFMAC* (Murshudov *et al.*, 1997) with working and free (5%) sets of data extended to include all data between 27.22 and 1.95 Å. The initial values for the *R* factor and $R_{\rm free}$ were 20.8 and 22.8%, respectively. Rounds of conjugate-gradient sparse-matrix refinement with bulk-solvent modelling according to the Babinet principle (Tronrud, 1996) were alternated with model verification using the program *O* (Jones *et al.*, 1991). Details of the final stage of the refinement are given in Table 2.

The NTA complex was treated in a similar manner to the 18 kDa fragment, except that the initial Fourier syntheses clearly showed a nitrilotriacetate molecule bound at the iron site and an associated movement of Tyr95. All data in the resolution range 26.9–1.9 Å were used and the initial values of the *R* factor and $R_{\rm free}$ were 19.2 and 20.8%, respectively; the final details of the refinement are given in Table 2.

2.4. Quality of the refined structures

A Ramachandran analysis as implemented in *PROCHECK* (Laskowski *et al.*, 1993) shows that 87.5% of the residues in the 18 kDa fragment lie in the most favoured regions, whilst 12.5% lie in the additionally allowed regions. The corresponding values for the NTA complex are 86.6 and 12.7%, respectively, with one residue lying in the generously allowed regions. This latter residue, Ser148, is part of a loop on the outside of the respective molecules comprising residues Glu142–Gly149. This loop, an insertion in the dOT sequence with respect to the hST sequence, is very poorly defined with fragmented electron density in both cases. In addition, there is no coherent electron density for the C-terminal residues Ala251 and Ala252 (Ala248 and Ala249 in hST) in the NTA complex.

3. Results and discussion

3.1. Overall molecular structure

The 18 kDa fragment corresponds to the second domain in the N-terminal lobe of duck ovotransferrin; the secondary structure of the fragment is represented by the ribbon diagram as shown in Fig. 1. Both the 18 kDa fragment and its NTA complex start at Ser94, but whereas the fragment clearly terminates at Ala252 (Ala249 in hST), the last two residues are not visible in the NTA complex. In both structures, the polypeptide chain adopts a very similar conformation to the NII domain of the rabbit and porcine serum transferrins (Hall *et al.*, 2002). Thus, some 150 C^{α} atoms of the 18 kDa fragment can be superimposed with an r.m.s. deviation of 0.78 Å on the corresponding atoms in the NII domain of porcine serum transferrin (pST).

3.2. Iron-binding sites

In the 18 kDa fragment, tyrosine residues Tyr95 and Tyr194 (Tyr188 in hST) and the bidentate carbonate anion coordinate to the ferric cation in a manner almost identical to that observed in the intact N-terminal lobe. The carbonate anion retains its intricate network of hydrogen bonds with the residues at the N-terminus of helix 5: Thr120 OG1, the guanidinium group of Arg124 and the main-chain NH groups of residues Ala126 and Gly127. It thereby effectively neutralizes the positive charge arising from the N-terminus of helix 5 and the arginine residue, whilst at the same time providing two oxygen ligands to the metal. However, a glycine residue has replaced Asp63 and His249 (hST numbering) that are present in the intact lobe and arise from domain NI and the second interdomain strand, respectively. This glycine residue, prob-

ably acquired during the proteolytic preparation of the domain NII fragment from the intact duck ovotransferrin molecule, binds to the iron through one of its carboxylate O atoms and its amino terminus (Fig. 2). Thus, it simulates the carboxylate group of the Asp63 and His249 NE2.

In the NTA complex, tyrosine Tyr194 (Tyr188 in hST) and the bidentate carbonate anion bind to the iron in a similar manner to the 18 kDa fragment and the intact transferrins. However, Tyr95 is displaced by the NTA moiety so that its hydroxyl O atom is some 3.8 Å away from the iron. In the place of Asp63, Tyr95 and His249 (hST numbering), the NTA binds to the iron through its carboxylate O atoms and the central N atom as shown in Fig. 3. However, the binding is not symmetric and one of the carboxylate O atoms and the central N atrom are 2.6 and 2.8 Å distant from the cation, respectively; the carboxylate group concerned is the most solvent exposed and also binds to solvent molecules. The NTA moiety appears to be neither fully bound to the cation nor fully released.

Details of the geometry of the iron sites in the 18 kDa fragment and its NTA complex are given in Table 3.[1]

3.3. Iron uptake by transferrins

It is not yet known physiologically in what form the iron is presented to apo transferrin or whether other enzymes such as ceruloplasmin are involved. However, kinetic studies have identified five principal steps in the formation of the specific metal–anion–transferrin ternary complex if the metal is added as a chelate complex (Aisen & Leibman, 1973; Cowart *et al.*, 1982). Initially, the carbonate (or bicarbonate) anion binds to the transferrin and this is followed by the removal of one or more ligands from the metal chelate. A quaternary transferrin–anion–metal–chelate complex is next formed and the remaining chelate ligands are then removed from the iron. Lastly, a conformational change occurs to form the final specific transferrin complex (see, for example, Baker, 1993). It is likely that the initial carbonate binding is facilitated by the positive charge at the anion-binding site in the inter-domain cleft, together with other exposed positively charged side chains in the cleft. The metal–chelate complex can then bind and an exchange of ligands take place with the two tyrosines, one in domain II and the other on a connecting strand, and the bidentate anion. Finally, binding can be completed by loss of the chelator and domain closure providing the final two ligands, histidine from the second connecting strand and aspartic acid from domain I. The structure of the 18 kDa fragment of duck ovotransferrin appears to be completely consistent with this scheme, representing in the absence of the glycine residue the situation immediately prior to domain closure.

However, the NTA complex appears even more interesting since it represents a specific quaternary transferrin–anion–metal–chelate complex and suggests that the ligation of the tyrosine residues is stepwise. The ferric chelate complex comprises the NTA bound in a tetradentate manner to the ferric cation through the central nitrogen and the three carboxyl groups, with two water molecules occupying the remaining positions in the octahedral coordination sphere. Binding of the carbonate anion at the N-terminus of helix 5 will be the first stage of the uptake process. Binding of the ferric cation then follows *via* the carbonate anion, in a bidentate manner, and Tyr188 (hST numbering) situated at the N-terminus of helix 7. Concomitantly, the Fe–NTA complex loses the two water ligands. Tyr95 does not appear to be involved at this stage and there appears in addition to be a partial dissociation of some of the metal–chelate bonds, so that the Fe—N(NTA) and Fe—O12(NTA) separations are significantly increased (see Table 3). In the intact protein, further dissociation of the metal–chelate linkages followed by the commencement of domain closure will result in the second tyrosine Tyr95 and His249 (hST numbering), both located on the strands connecting the two domains in the lobe, binding to the iron. Finally, after complete removal of the NTA chelator from the protein environment, domain closure causes Asp63

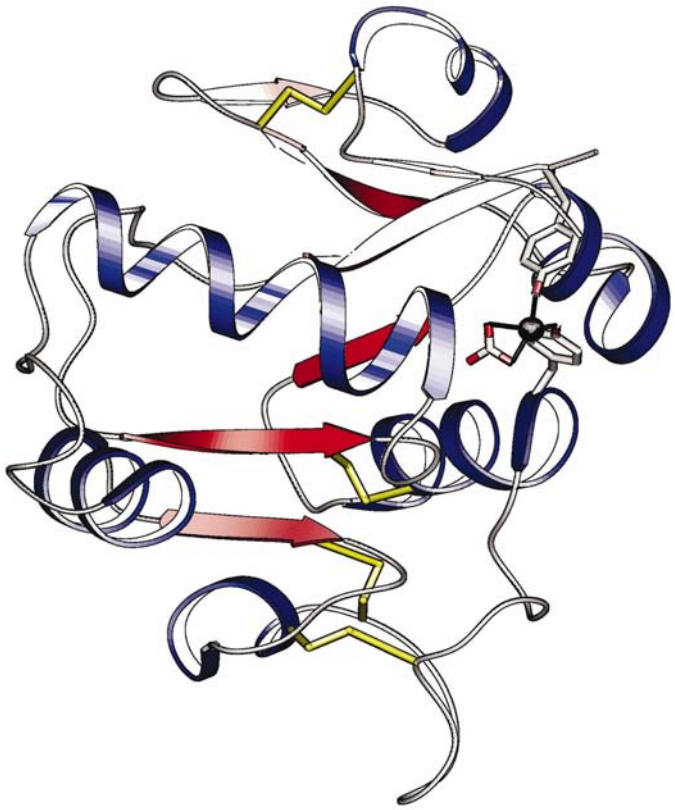

Figure 1
A ribbon diagram of the 18 kDa fragment of duck ovotransferrin corresponding to the NII domain. The location of the synergistic carbonate anion and the ferric cation at the N-terminus of the helix formed by residues 124–134, helix 5, is clearly shown together with tyrosine residues Tyr95 and Tyr188. The remaining ligands to the iron have been omitted (see Figs. 2 and 3), but the exposure of the cation to the solvent is apparent. The poorly defined loop region, 144–149, is at the left-hand side of the diagram, immediately following helix 5.

[1] Supplementary data have been deposited in the IUCr electronic archive (Reference: ad0168). Services for accessing these data are described at the back of the journal.

in domain NI to bind to the iron. A similar scheme will apply to iron binding in the C-terminal lobe of the transferrins.

The aspartic acid Asp63 is likely to be the last ligand to bind to the iron as domain closure occurs. However, its role has been the subject of debate, with a suggestion that it may even trigger domain closure (Grossmann *et al.*, 1993). It is the only ligand from domain I and also forms at least one important inter-domain hydrogen bond. Mutations at or near the aspartic acid are associated with impairment of iron binding. Thus, a natural variant of human serum transferrin in which a glycine

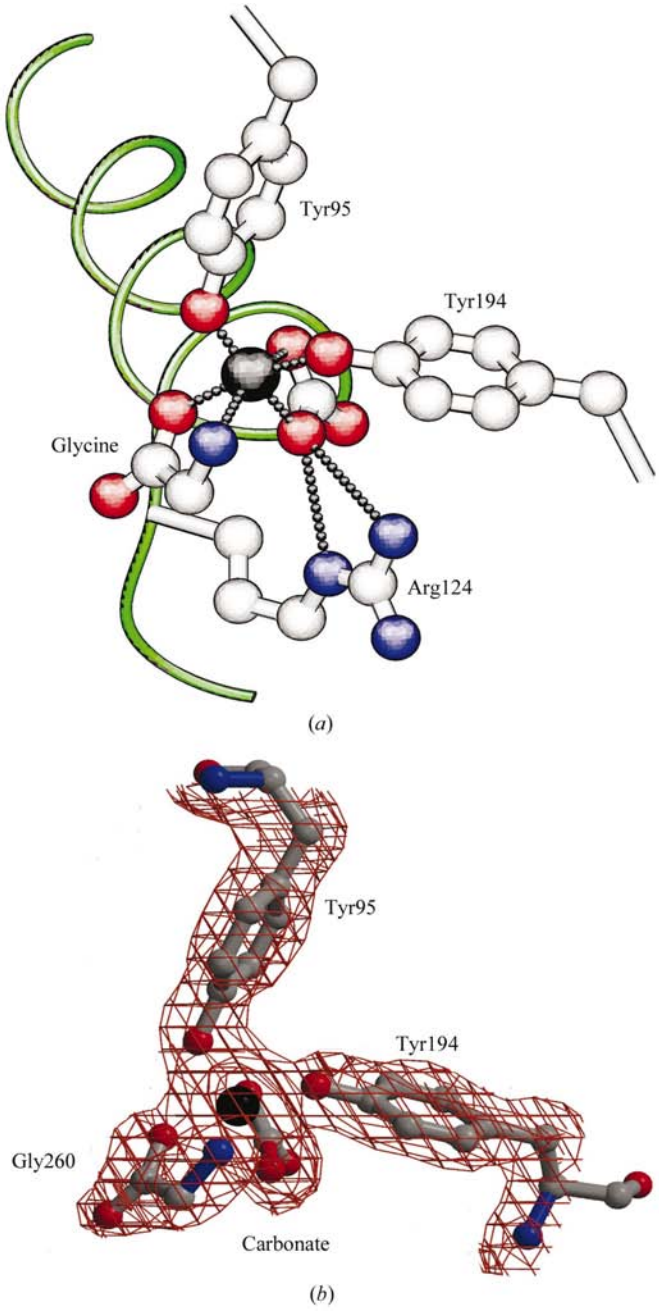

Figure 2
(*a*) The Fe^{III}-binding site in the 18 kDa fragment of duck ovotransferrin. The site is identical to that in the intact protein, except that the aspartic acid and histidine residues are replaced by a glycine adventitiously acquired during the preparative proteolysis. (*b*) The electron density in a $2|F_o| - |F_c|$ synthesis in the vicinity of the Fe atom, contoured at the 1 r.m.s. level.

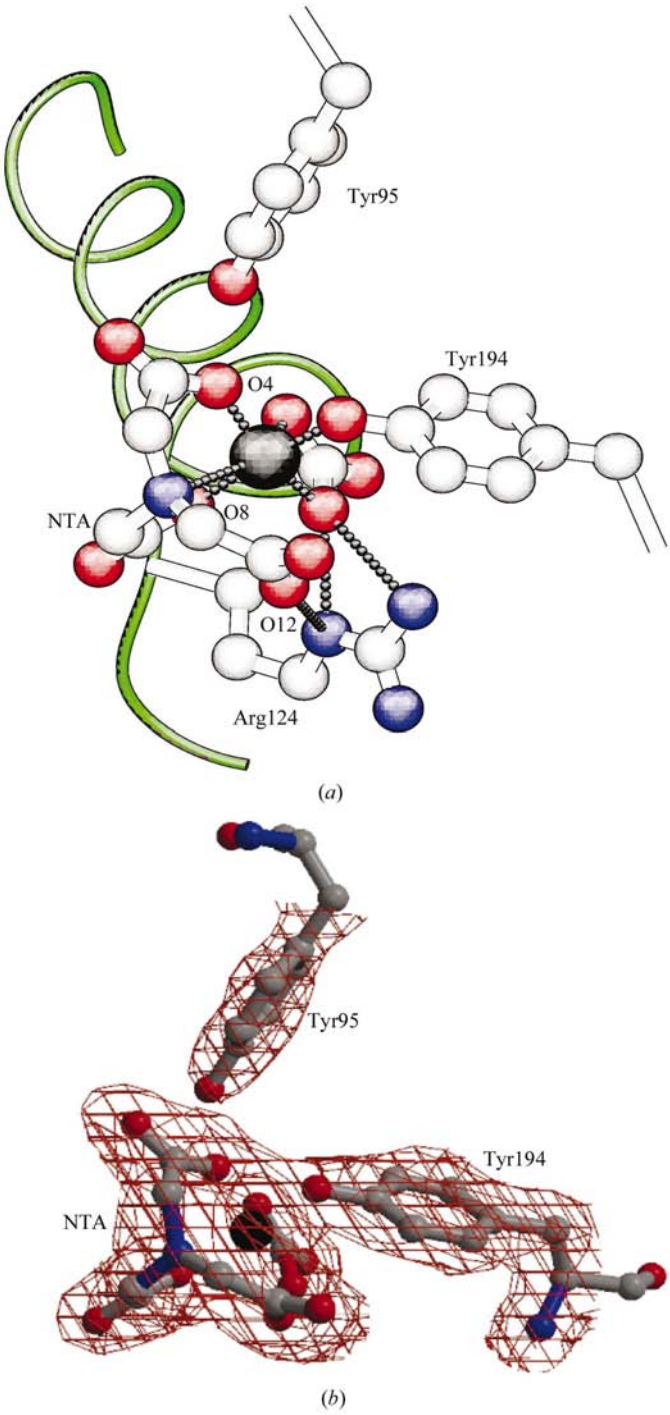

Figure 3
(*a*) The iron-binding site in the nitrilotriacetate (NTA) complex of the 18 kDa duck ovotransferrin fragment. The iron binds to the carbonate anion and to one of the tyrosine residues, Tyr194 (188 in hST numbering). The second tyrosine, Tyr95, on a connecting strand between the two domains, is some 3.8 Å away from the iron. The NTA binds tightly to the iron through the carboxyl O atoms O4 and O8; the central N atom and the third carboxylate group provide more weakly bound ligands and the Fe—O12 linkage is not included in the figure. This carboxylate group also binds to solvent molecules. (*b*) The electron density in a $2|F_o| - |F_c|$ synthesis in the vicinity of the Fe atom, contoured at the 1 r.m.s. level.

Table 3
Geometry of binding sites in the 18 kDa fragment, its NTA complex and and porcine serum transferrin; hST numbering is used throughout the table.

(*a*) Bond lengths (Å).

18 kDa fragment		NTA complex		pST: N-lobe	
				Fe—OD1 (Asp63)	2.1
Fe—OH1 (Tyr95)	1.9			Fe—OH1 (Tyr95)	2.0
Fe—OH1 (Tyr188)	2.0	Fe—OH1 (Tyr188)	1.9	Fe—OH1 (Tyr188)	1.8
				Fe—NE2 (His249)	2.2
Fe—O2 (carbonate)	2.1	Fe—O2 (carbonate)	2.1	Fe—O2 (carbonate)	2.1
Fe—O3 (carbonate)	2.0	Fe—O3 (carbonate)	2.1	Fe—O3 (carbonate)	2.2
Fe—O (Gly260)	1.9	Fe—O4 (NTA)	1.7		
Fe—N (Gly260)	2.1	Fe—O8 (NTA)	2.1		
		Fe—O12 (NTA)	2.6		
		Fe—N (NTA)	2.8		

(*b*) The metal-synergistic carbonate anion bond lengths (Å) and the associated hydrogen-bond network.

Network	18 kDa	NTA	pST: N-lobe
O1—OG (Thr120)	2.6	2.5	2.7
O1—N (Gly127)	2.9	2.8	2.9
O2—N (Ala126)	2.6	2.8	2.8
O2—OH1 (Tyr95)	—	3.2	—
O2—Fe	2.2	2.1	2.1
O3—NE (Arg124)	3.0	2.6	2.8
O3—NH2 (Arg124)	3.2	2.9	2.9
O3—Fe	2.0	2.1	2.2

residue two residues away from the aspartic acid in the C-lobe is changed to an arginine shows reduced iron binding (Evans *et al.*, 1988). This observation has been explained by the formation of an ion pair between the arginine and the aspartate (Lindley *et al.*, 1993). In addition, the Asp→Ser mutation in the C-lobe of melanotransferrin has been associated with a complete loss of iron binding (Baker *et al.*, 1992). However, structural studies on the Asp60Ser mutant of the N-lobe of human lactoferrin suggest that the aspartic acid residue serves only as part of a lock that holds the domains closed when iron is bound (Faber *et al.*, 1996). In the structure of the Asp60Ser mutant the serine binds to the iron though a solvent molecule, which in turn participates in inter-domain hydrogen bonding. However, the two domains in the N-lobe of the Asp60Ser mutant are even closer together than in the native molecule. The absence of the aspartic acid alone does not appear to prohibit iron binding and the behaviour of the C-lobe of melanotransferrin must result from a combination of mutations that destabilize the anion-binding site as well as the iron binding.

4. Conclusions

The structures of the 18 kDa NII domain fragment of duck ovotransferrin and its NTA fragment fully support a mechanism of iron uptake by the transferrins that involves initial binding of the carbonate anion followed by the formation of specific ternary metal–anion–transferrin and quaternary transferrin–anion–metal–chelate complexes prior to loss of the chelator and domain closure.

The authors would like to acknowledge the provision of synchrotron facilities at the SRS, Daresbury Laboratory by the Central Laboratory of the Research Councils in the UK. They also acknowledge the Medical Research Council, the Biotechnology and Biological Sciences Research Council and the Engineering and Physical Sciences Research Council for supporting the Structural Biology Group at Daresbury Laboratory. They are pleased to thank Dr C. Joannou for helpful discussions and the Guy's and St Thomas' Charitable Trust for partial support to MLH. Fig. 1 was created with the *SETOR* suite of programs (Evans, 1993), whereas Figs. 2 and 3 were drawn with the help of *MolScript* (Kraulis, 1999), *BobScript* (Esnouf, 1999) and *Raster3D* (Merritt & Bacon, 1997).

References

Aisen, P. (1998). *Metal Ions in Biological Systems*, Vol. 35, edited by A. Sigel, pp. 585–531. New York: Marcel Dekker.
Aisen, P. & Leibman, A. (1973). *Biochim. Biophys. Acta*, **304**, 797–804.
Arnesano, F. & Provenzani, A. (2001). *Handbook on Metalloproteins*, Vol. 12, edited by I. Bertini, A. Sigel & H. Sigel, pp. 571–594. New York: Marcel Dekker.
Baker, E. N. (1993). *Perspectives on Bioinorganic Chemistry*, Vol. 2, edited by R. W. Hay, J. R. Dilworth & K. B. Nolan, pp. 161–205. Greenwich, CT, USA: JAI Press.
Baker, E. N., Baker, H. M., Smith, C. A., Stebbins, M. R., Kahn, M., Hellstrom, K. E. & Hellstrom, I. (1992). *FEBS Lett.* **298**, 215–218.
Collaborative Computational Project, Number 4 (1994). *Acta Cryst.* D**50**, 760–763.
Cowart, R. E., Kojima, N. & Bates, G. W. J. (1982). *J. Biol. Chem.* **257**, 7560–7565.
Crichton, R. R. (2001). *Inorganic Biochemistry of Iron Metabolism*, 2nd ed. London: Ellis Horwood.
Cruickshank, D. W. J. (1996). *Proceedings of the CCP4 Study Weekend. Macromolecular Refinement*, edited by E. Dodson, M. Moore, A. Ralph & S. Bailey, pp. 11–22. Warrington: Daresbury Laboratory.
Esnouf, R. M. (1999). *Acta Cryst.* D**55**, 938–940.
Evans, R. W. & Madden, A. D. (1984). *Biochem. Soc. Trans.* **12**, 661–662.
Evans, R. W., Meilak, A., Aitken, A., Patel, K. J., Wong, C., Garratt, R. C. & Chitnavis, B. (1988). *Biochem. Soc. Trans.* **16**, 834–835.
Evans, S. V. (1993). *J. Mol. Graph.* **11**, 134–138.
Faber, H. R., Bland, T., Day, C. L., Norris, G. E., Tweedie, J. W. & Baker, E. N. (1996). *J. Mol. Biol.* **256**, 352–363.
Grossmann, J. G., Mason, A. B., Woodworth, R. C., Neu, M., Lindley, P. F. & Hasnain, S. S. (1993). *J. Mol. Biol.* **231**, 554–558.
Hall, D. R., Hadden, J. M., Leonard, G. A., Bailey, S., Neu, M., Winn, M. & Lindley, P. F. (2002). *Acta Cryst.* D**58**, 70–80.
Jandl, J. H., Inman, J. K., Simmons, R. L. & Allen, D. W. (1959). *J. Clin. Invest.* **38**, 161–185.
Jones, T. A., Zou, J. Y., Cowan, S. W. & Kjeldgaard, M. (1991). *Acta Cryst.* A**47**, 110–119.
Kraulis, P. J. (1999). *J. Appl. Cryst.* **24**, 946–950.
Laskowski, R. A., MacArthur, M. W., Moss, D. S. & Thornton, J. M. (1993). *J. Appl. Cryst.* **26**, 283–291.
Leslie, A. (1991). *Crystallographic Computing V*, edited by D. Moras, A. D. Podjarny & J. C. Thierry, pp. 27–38. Oxford University Press.
Lindley, P. F. (2001). *Handbook of Metalloproteins*, Vol. 2, edited by A. Messerschmidt, R. Huber, T. Poulos & K. Weighardt, pp. 793–811. Chichester: John Wiley & Sons.

Lindley, P. F., Bajaj, M., Evans, R. W., Garratt, R. C., Hasnain, S. S., Jhoti, H., Kuser, P., Neu, M., Patel, K., Sarra, R., Strange, R. & Walton, A. (1993). *Acta Cryst.* D**49**, 292–304.
Matthews, B. W. (1968). *J. Mol. Biol.* **33**, 491–497.
Merritt, E. A. & Bacon, D. J. (1997). *Methods Enzymol.* **277**, 505–524.
Murshudov, G. N., Vagin, A. A. & Dodson, E. J. (1997). *Acta Cryst.* D**53**, 240–255.
Smith, C. A. (2001). *Handbook of Metalloproteins*, Vol. 2, edited by A. Messerschmidt, R. Huber, T. Poulos & K. Weighardt, pp. 812–833. Chichester: John Wiley & Sons.
Tronrud, D. (1996). *Proceedings of the CCP4 Study Weekend. Macromolecular Refinement*, edited by E. Dodson, M. Moore, A. Ralph & S. Bailey, pp. 1–10. Warrington: Daresbury Laboratory.